Permafrost carbon-climate feedbacks accelerate global warming

Charles D. Koven[a,b,1], Bruno Ringeval[a], Pierre Friedlingstein[c], Philippe Ciais[a], Patricia Cadule[a], Dmitry Khvorostyanov[d], Gerhard Krinner[e], and Charles Tarnocai[f]

[a]Laboratoire des Sciences du Climat et de l'Environnement, Centre National de la Recherche Scientifique/Commissariat à l'Energie Atomique, 91191 Gif-sur-Yvette, France; [b]Earth Sciences Division, Lawrence Berkeley National Laboratory, Berkeley, CA 94720; [c]College of Engineering, Mathematics and Physical Sciences, University of Exeter, Exeter EX4 4QF, United Kingdom; [d]Laboratoire de Météorologie Dynamique, École Polytechnique, 91128 Palaiseau, France; [e]Laboratoire de Glaciologie et Géophysique de l'Environnement, Centre National de la Recherche Scientifique/Université Joseph Fourier, Grenoble 1, Unité Mixte de Recherche 5183, F-38402 Grenoble, France; and [f]Agriculture and Agri-Foods Canada, Ottawa, ON, Canada K1A 0C5

Edited* by Inez Y. Fung, University of California, Berkeley, CA, and approved July 12, 2011 (received for review March 24, 2011)

Permafrost soils contain enormous amounts of organic carbon, which could act as a positive feedback to global climate change due to enhanced respiration rates with warming. We have used a terrestrial ecosystem model that includes permafrost carbon dynamics, inhibition of respiration in frozen soil layers, vertical mixing of soil carbon from surface to permafrost layers, and CH_4 emissions from flooded areas, and which better matches new circumpolar inventories of soil carbon stocks, to explore the potential for carbon-climate feedbacks at high latitudes. Contrary to model results for the Intergovernmental Panel on Climate Change Fourth Assessment Report (IPCC AR4), when permafrost processes are included, terrestrial ecosystems north of 60°N could shift from being a sink to a source of CO_2 by the end of the 21st century when forced by a Special Report on Emissions Scenarios (SRES) A2 climate change scenario. Between 1860 and 2100, the model response to combined CO_2 fertilization and climate change changes from a sink of 68 Pg to a 27 ± 7 Pg sink to 4 ± 18 Pg source, depending on the processes and parameter values used. The integrated change in carbon due to climate change shifts from near zero, which is within the range of previous model estimates, to a climate-induced loss of carbon by ecosystems in the range of 25 ± 3 to 85 ± 16 Pg C, depending on processes included in the model, with a best estimate of a 62 ± 7 Pg C loss. Methane emissions from high-latitude regions are calculated to increase from 34 Tg CH_4/y to 41–70 Tg CH_4/y, with increases due to CO_2 fertilization, permafrost thaw, and warming-induced increased CH_4 flux densities partially offset by a reduction in wetland extent.

carbon cycle | land surface models | cryosphere | soil organic matter | active layer

Boreal and Arctic terrestrial ecosystems are particularly sensitive to future warming (1). These cold regions are crucial to the global carbon cycle because they are rich in soil organic carbon, which has built up in frozen soils, litter, and peat layers. Laboratory incubation experiments (2) and field studies (3) suggest that this old carbon could be lost rapidly through decomposition in response to warming. In particular, the slow burial of soil carbon below the base of seasonally thawed surface layers (the active layer) into deeper permafrost layers has led over tens of millennia to the formation of an enormous stock. This carbon stock is presently not actively cycling, but might become available for respiration if frozen soils thaw. Estimates of the total northern carbon pool are 495 Pg for the top meter of soils, 1,024 Pg to 3 m, and an additional 648 Pg for deeper carbon stored in yedoma (frozen, carbon-rich sediments) and alluvial deposits (4). Such a huge permafrost carbon pool, formed during the Pleistocene and Holocene, exists because decomposition is strongly inhibited in frozen soils, thus allowing old, otherwise labile carbon to persist and accumulate slowly to the present.

In the recent Coupled Carbon-Climate Change Model Intercomparison Project (C^4MIP) (5)—which formed the estimate for the strength of the carbon-climate feedback for the Intergovernmental Panel on Climate Change Fourth Assessment Report (IPCC AR4) (6, 7)—and other studies (e.g., ref. 8) that examine the effects of CO_2 fertilization and climate change on the net carbon balance of terrestrial and ocean ecosystems, most terrestrial biosphere models predicted an enhanced carbon sink due to warming in high latitudes (Fig. 1*D*) (9), through longer growing seasons and enhanced productivity that offsets the warming-induced increase in heterotrophic respiration. However, none of these coupled models accounted for carbon vulnerable to decomposition when permafrost thaws. Models that have considered permafrost carbon losses calculate total emissions of CO_2 from permafrost carbon from 7–17 Pg by 2100 (10) to 190 ± 64 Pg by 2200 (11). In addition to frozen soil carbon, northern wetlands are a strong source of methane (CH_4) to the atmosphere, averaging 35–45 Tg CH_4/y (12, 13), and this methane source is sensitive to changes in permafrost, wetlands hydrology, and ecosystem productivity. None of the models of C^4MIP accounted for the climate feedbacks of natural CH_4 sources, even though CH_4 is a very efficient greenhouse gas [global warming potential (GWP) = 25] on 100 y timescale) (14).

Model

We selected the ORCHIDEE model as a representative land component of the C^4MIP models, and designed four separate sets of simulation experiments to explore the sensitivity of the northern high-latitude CO_2 and CH_4 balance to the inclusion of critical soil carbon processes (Table S1). Typically, soil carbon models have used either a single bulk vertically integrated soil pool, though (10) adapted this approach to high latitudes by normalizing the carbon of this single pool relative to the thickness of the active layer. Here, in all cases, we use a fully vertically discretized soil carbon module, recently developed (15), where decomposition rates are calculated for each soil level, to dynamically model the steep vertical gradient in soil carbon residence time that occurs at the permafrost table in permafrost-affected soils (Fig. S1). In addition, the model soil physics has been improved to more realistically capture the effects of organic matter on active layer thickness (15).

The four experiments explored here are (*i*) control, in which soil carbon is vertically resolved but no additional processes are added; (*ii*) freeze, inhibition of decomposition in seasonally frozen soil layers, but no soil carbon in permafrost soil layers; (*iii*) permafrost, inclusion of permafrost carbon through vertical

Author contributions: C.D.K., B.R., P.F., and P. Ciais designed research; C.D.K., B.R., P.F., P. Ciais, P. Cadule, D.K., G.K., and C.T. performed research; C.D.K., B.R., P.F., P. Ciais, P. Cadule, D.K., G.K., and C.T. analyzed data; and C.D.K., B.R., P.F., P. Ciais, and G.K. wrote the paper.

The authors declare no conflict of interest.

*This Direct Submission article had a prearranged editor.

[1]To whom correspondence should be addressed. E-mail: cdkoven@lbl.gov.

This article contains supporting information online at www.pnas.org/lookup/suppl/doi:10.1073/pnas.1103910108/-/DCSupplemental.

ENVIRONMENTAL SCIENCES

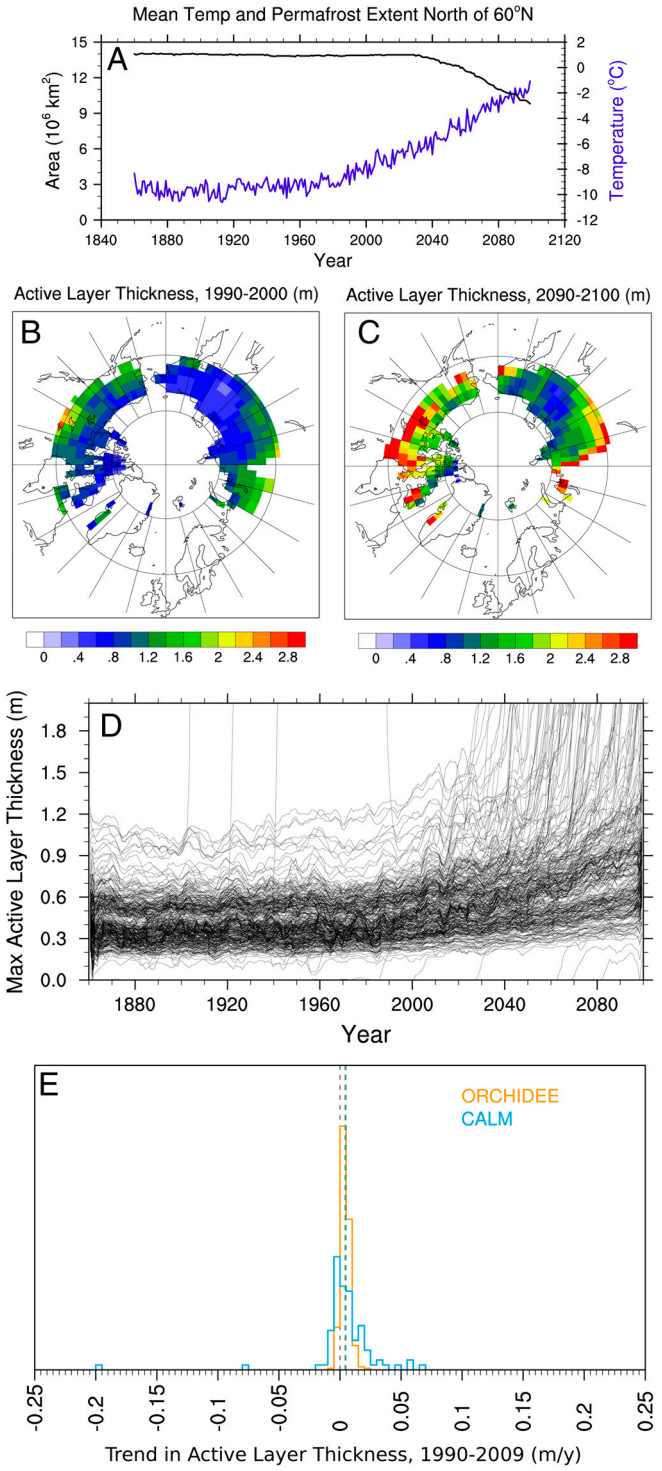

Fig. 1. Change in permafrost extent and properties over the model simulation period, for the region 60°N–90°N. (*A*) Black line, permafrost extent (to 50 m); blue line, mean annual temperature for the high-latitude terrestrial region. (*B*) Active layer thickness (maximum depth of seasonally thawed soils), 1990–2000. (*C*) Active layer thickness, 2090–2100. Blank grid cells in (*B*–*C*) are those where we do not calculate permafrost within the top 50 m. (*D*) Trends in active layer thickness for all permafrost grid cells in the model. (*E*) A histogram of modeled and observed [CALM, (25)] active layer thickness trends (m/y) based on regression over the period 1990–2009.

mixing and soil organic insulation (15); and (*iv*) heat, inclusion of microbial heat release by decomposing microbes to the soil thermal budget (16).

In addition to the CO_2 balance, we model the climate response of CH_4 natural emissions by both deep permafrost layers and wetlands. For deep permafrost, we incorporate in ORCHIDEE the detailed process-based model of (16), in which (*i*) methanogenesis can occur in oxygen-poor deep permafrost horizons, and methanotrophy in the aerated upper soil profile; (*ii*) soil gas (O_2 and CH_4) diffusion is calculated to trigger methanotrophy vs. aerobic decomposition; and (*iii*) heat release due to exothermic decomposition reactions (decomposition, methanogenesis, and methanotrophy) can be included in the soil thermal budget.

For CH_4 emissions by wetlands in regions outside permafrost areas and in upper soil layers of permafrost regions, we use the wetland-CH_4 enabled version of ORCHIDEE (17, 18), in which wetland extent (saturated soil fraction) is calculated prognostically using the TOPMODEL (19, 20) subgrid approach, and methane emission rates are calculated for a given wetland extent, following an approach similar to Walter et al. (21). We model the temperature sensitivity of methanogenesis using a Q_{10} of 3, relative to an initial location-dependent mean annual temperature T_{mean}, based on a site-level optimization (17). We calculate two separate sets of wetland CH_4 fluxes, one allowing the base T_{mean} to change with changing climate, and the other where T_{mean} remain fixed, to bracket the uncertainty associated with possible microbial decomposition adaptation to warming. Wetland simulations are also calculated with separate biochemical CO_2 fertilization effect alone, and with the combined fertilization and climate effect of CO_2. We then add these CH_4 flux distributions across the high latitudes to the deep permafrost CH_4 emissions calculated from the permafrost model, to obtain total high-latitude natural CH_4 emissions.

In each simulation experiment a new mechanism is added to test its effect on the modeled CO_2 balance. The control case uses the standard ORCHIDEE soil carbon temperature sensitivity to respiration, with a classic temperature sensitivity Q_{10} of two (ref. 5). In the freeze experiment, we inhibit soil carbon decomposition by seasonal freezing (different sensitivity functions of low frozen respiration rate to warming were tested; see SI Text and Fig. S2). In the control and freeze cases, there is no vertical movement of soil carbon; thus no permafrost carbon stocks exist in these simulations. In the permafrost experiment, we add an initial permafrost carbon pool beneath the active layer by including thermal insulation by soil carbon and cryoturbation as in ref. 15; this mixing leads to the downward movement and burial of soil carbon from seasonally thawed soil layers into the upper permafrost (to ~3 m, Fig. S3), allowing a realistic model initialization. In addition, the specific very thick permafrost loess deposits in yedoma areas are initialized prior to the 10,000-y model equilibration with uniform carbon concentrations below the active layer to match observed carbon stocks (4) to include the presence of this relic frozen-but-labile Pleistocene carbon, mainly over Eastern Siberia. Finally, in the heating experiment, the soil thermal budget of the model accounts for the exothermic heat released by decomposition, exactly as described by ref. 16. We estimate uncertainty of each process using an ensemble of runs and varying key parameters over a given range.

We perform all model simulations over the period 1860–2100. For each experiment, we calculate a control run with preindustrial CO_2 levels and climate, a CO_2-only run with increasing CO_2 but fixed climate, and a CO_2+ climate run where both CO_2 concentration and climate vary. We calculate the effect of CO_2 (Fig. 2*C*) as the difference between the CO_2-only and the control runs, and the effect of climate change (Fig. 2*D*) as the difference between the CO_2+ climate and the CO_2-only runs. For all experiments, we run ORCHIDEE offline, so that each experiment is forced by the same meteorology. The model is forced by climate fields constructed as a base climatology (22, 23) plus anomalies relative to a climatological period 1961–1990 of the Institut Simon Pierre Laplace Climate Model 4 climate system model

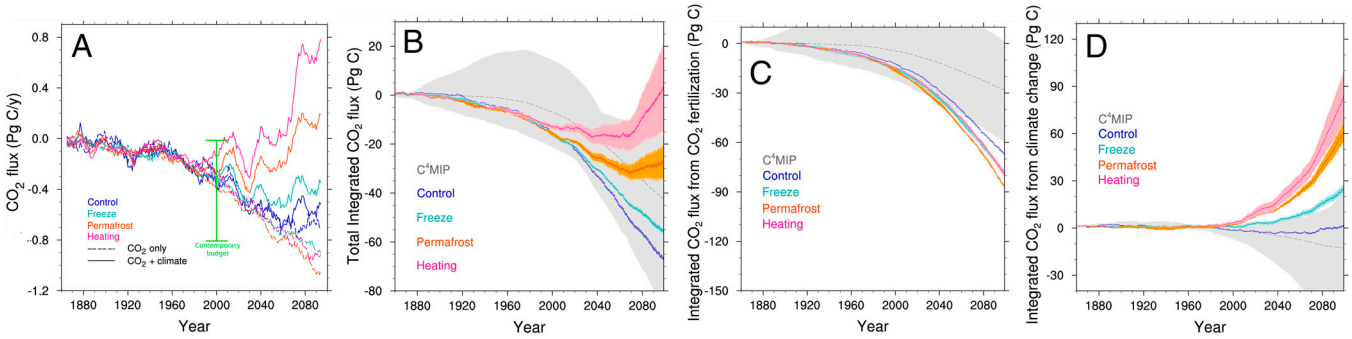

Fig. 2. Change in carbon fluxes over the model run. (*A*) Mean fluxes over modeled period. Contemporary budget estimate from McGuire et al. (1) (*B*) integrated changes. (*C*) Integrated changes in carbon balance due to rising CO_2 concentration alone. (*D*) Integrated change in carbon balance due to climate change alone (difference between CO_2-only and CO_2+climate change).

(24) for prescribed greenhouse gas-forced historical and future [Special Report on Emissions Scenarios (SRES) A2].

Results and Discussion

For each experiment, the initial equilibrium soil carbon stocks differ as a result of the processes included (Fig. S4 and Table S1), with a large increase in high-latitude soil C stocks (from ~200 Pg to ~500 Pg C in the top 3 m of soil) from permafrost processes, leading to better agreement with soil carbon observations (4) in freeze and permafrost, however, a substantial underestimate of initial carbon stocks still exists because we do not model the buildup of peatlands or organic soils.

We run the ORCHIDEE model fitted with these processes added in a transient climate change scenario. The modeled climate response leads to significant warming at high latitudes (Fig. 1), with mean high-latitude surface soil temperature rising approximately 8 C by 2100—much larger than the global mean—and permafrost extent (within the top 3 m) reduced by 30%. In addition, where permafrost does still exist at 2100, the active layer is deepened, with consequent thawing of previously frozen carbon. The changes in permafrost properties have a lag with respect to surface warming, and changes in active layer depth over the observed period (1990–2009) are small (mean 0.5 cm/y) and agree well with observed changes in active layer thickness (25), which we calculate by linear regression of all circumpolar active layer monitoring network (CALM) sites poleward of 60°N.

The modeled carbon fluxes of the region north of 60°N (Fig. 2) change as a result of both the effect of CO_2 fertilization on photo-

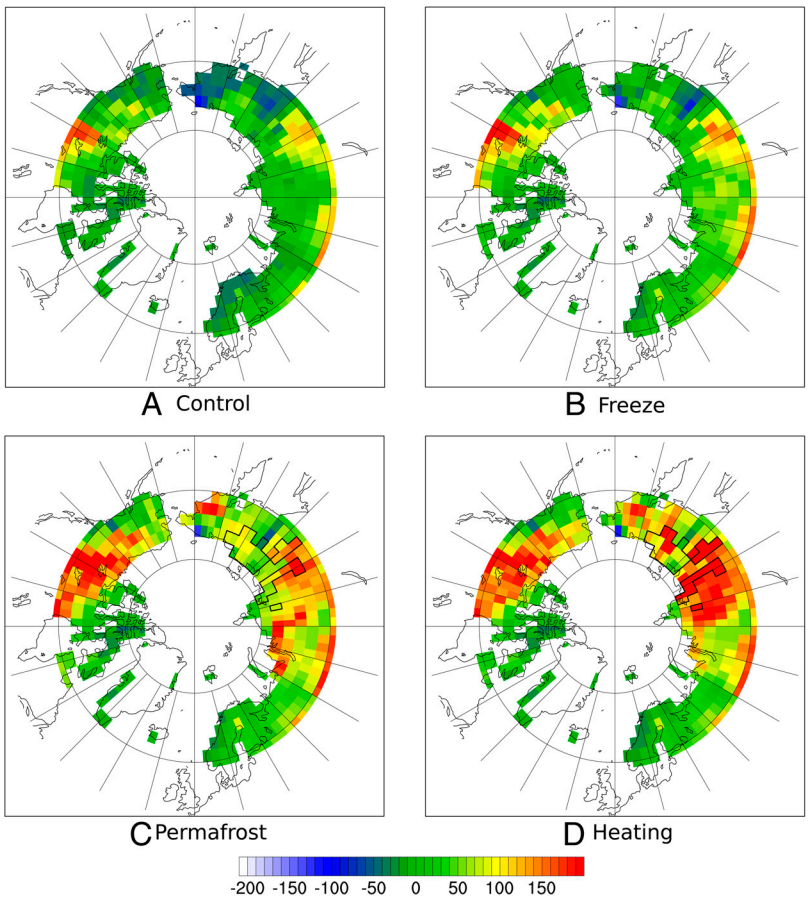

Fig. 3. Spatial patterns of net CO_2 fluxes due to climate change at end of 21st century, for (*A*) control, (*B*) freeze, (*C*) permafrost, and (*D*) heating experiments. Units are in gC/m2/y. Outlined cells are initialized as containing deep yedoma carbon.

synthesis, and the warming due to climate change. In all experiments, the effect of CO_2 fertilization is to increase vegetation productivity and thus create a carbon sink of 69–88 Pg relative to the control, whereas that of climate change is a net loss of carbon relative to the CO_2-only case, whose magnitude differs strongly between experiments. We also show the model range for the C^4MIP experiments in Fig. 2 *C* and *D*, with a cumulative sink ranging from 0 to 60 Pg (mean 29 Pg) due to CO_2 fertilization alone, and from a sink of 77 Pg to a source of 20 Pg (mean 14 Pg sink) due to warming. The uncertainty evidenced by the large spread between the C^4MIP models relates to their different parameterizations, their initial carbon storage as well as their remaining climate drifts (due to low-frequency variance and initial model disequilibrium), and associated drifts in the carbon fluxes. ORCHIDEE shows a very high sensitivity to CO_2 fertilization at high latitudes; this high sensitivity is likely due to a number of biases in the model: (*i*) there is no limitation by N in the model, and thus increases in CO_2 directly allow increases in productivity; and (*ii*) the baseline productivity of ORCHIDEE at high latitudes is higher than other models (26, 27), thus a proportionally similar change in the productivity leads to a larger gross change. These issues are also evident in the CH_4 emissions, which show a high sensitivity to CO_2 fertilization through substrate availability and local hydrologic feedbacks (18). Future work to integrate a dynamic N cycle and improve soil hydrology should reduce these biases. The sensitivity to CO_2 fertilization increases further in the model experiments because the longer turnover times of soil carbon with permafrost processes lead to a greater capacity for changes in productivity to translate to changes in storage.

In the control case given the ORCHIDEE model, the effect of warming is to lead to a large increase in vegetation productivity through longer growing seasons (+37 d over 1990–2100) that offsets the increase in heterotrophic respiration during the 21st century. Thus, this simulation gives only a small loss due to warming of 1 Pg C by 2100, a result within the range of C^4MIP models (5), as seen in Fig. 2*D*. In the freeze experiment, the larger initial soil carbon stocks and higher effective temperature sensitivity of decomposition lead to a cumulative source due to warming of $25(+-3)$ Pg, which occurs mainly in the spring and fall (Fig. S5) due to a lengthened unfrozen soil carbon decomposing season (to a mean of 165 d relative to 130 d in 1990). The permafrost experiment gives an even larger cumulative source of CO_2 of $62(+-6)$ Pg due to warming over the 21st century. This carbon source is caused by partial decomposition of the old permafrost carbon pool, with the largest changes in the summer. Lastly, in the heating experiment, the extensive thawing of permafrost carbon stocks is accelerated by soil microbes releasing heat within the bottom of the active layer, which leads to a cumulative carbon loss due to warming of $85(+-16)$ Pg. We note that the warming-induced carbon loss also begins earlier in the experiment with microbial heating (Fig. 2*A*), leading to a contemporary high-latitude carbon sink that is small, but within the range of regional estimates (1). In the permafrost case, which does not include the heating term, Arctic ecosystems shift from a CO_2 fertilization-driven sink to a climate change-driven source before 2100.

Fig. 3 shows the spatial distribution of the climate-induced CO_2 flux anomalies for each of the model experiments during the period 2090–2100. The control case shows widespread sink, which is partially attenuated in the freeze case. In the permafrost and heating cases, the region becomes a net source, with CO_2 emissions highest in regions that lie at the margins of the current permafrost zone, where permafrost is lost or the active layer substantially deepened in the future. Large carbon losses are seen in central Canada for the permafrost experiment, where substantial permafrost stocks exist that are vulnerable to warming. The effect of the microbial heat release in the heating experiment is particularly strong in Eastern Siberia, where it leads to more rapid permafrost degradation and associated carbon loss than is calculated in the permafrost experiment. The yedoma carbon stocks do not substantially contribute to the CO_2 or CH_4 fluxes in the permafrost case, because they are located in the coldest regions of Siberia, which are the most stable with respect to warming and thus have not thawed to depth by 2100 in this simulation.

Fig. 4 and Table S2 show the CH_4 balance for the permafrost and heating cases, also accounting for CH_4 emissions from wetlands. The effect of CO_2 fertilization is to increase the productivity of wetland plants and thus the methanogenesis substrate, leading to increased CH_4 emissions, to 71–74 Tg/y from 34 Tg/y in the early 20th century; this model estimate is subject to the same biases as for the larger carbon cycle, and has large uncer-

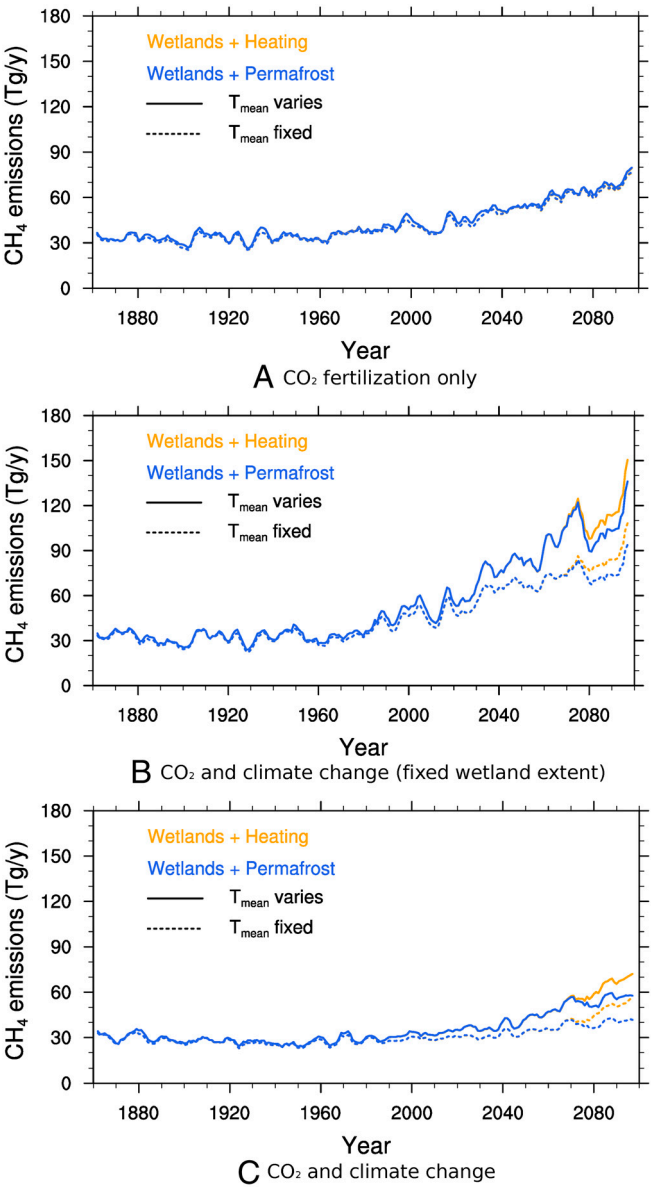

Fig. 4. CH_4 fluxes from high-latitude region over model runs (Tg CH_4). (*A*) CH_4 emissions under CO_2 fertilization alone; (*B*) CH_4 emissions under combined CO_2 increase and climate change, but holding wetland extent fixed; (*C*) CH_4 emissions under full climate change experiment with CO_2, climate, and its effect on wetland extent all varying. For each case, two separate wetland CH_4 experiments were carried out, with the reference temperature for methanogenesis, T_{mean}, remaining fixed or changing with climate. In addition, two separate permafrost CH_4 experiments were carried out, corresponding to the permafrost and heating experiments for the carbon balance.

tainties. Including warming as well, but holding wetland extent fixed, leads to enhanced emissions of 84–120 Tg/y, with the large value for the runs in which T_{mean} is held fixed. However, warming leads in our wetland hydrology model to a reduction of wetland area due to increased evapotranspiration, leading to less summer inundation and thus less CH_4 emission, for an increase to only 41–57 Tg/y. A similar shrinking of Arctic lakes has already been observed (28, 29), however this term is a large source of uncertainty in the CH_4 model. In the permafrost simulation, the deep permafrost carbon stores that could serve as the basis for extra methane emissions (16) are thawed only partially and in their upper layers in the time frame considered, thus not leading to large upland permafrost CH_4 emissions. Therefore, the change in CH_4 emissions is almost entirely realized from changes of wetland areas and flux intensity. By contrast, in the heating simulation, a fraction of 0–30% of deep permafrost thaws by the self-heating feedback that is described by ref. 16, leading to extramethanogenesis because of the deeper yedoma permafrost carbon that is decomposed. This switch on of deep permafrost methanogenesis leads to an additional methane source of up to 14 Tg CH_4/y, 40% of the current total high-latitude CH_4 natural source (gas hydrates nonmodeled) although with large uncertainties. Using a CH_4 GWP of 25 and summing the changes to the integrated CO_2 and CH_4 budgets over the scenario with fixed methanogenesis T_{mean} leads to a change in the high-latitude GWP of −63 Pg C-equivalent for the control case and −22 Pg C-equivalent for the permafrost case. However, climate change alone induces an increase in GWP of the region of 47 Pg C-equivalent for the permafrost case.

The version of ORCHIDEE used here for testing the sensitivity of high-latitude CO_2 and CH_4 fluxes to warming does not include C-N interactions, which may affect both the CO_2-fertilization and climate response to plant growth (30, 31). In particular, mineralization of nitrogen from thawing permafrost soil organic matter could lead to both enhanced plant growth and decomposition, with an uncertain sign on the net carbon balance response to the added N (32, 33). Inclusion of these interactions in ORCHIDEE without permafrost representation (18) leads to almost cancellation of the high-latitude carbon sink due to CO_2 fertilization. By contrast, when including C-N interactions and warming, the balance at high latitudes between increased growth and respiration is only shifted slightly. Including C-N interactions in our simulations should strongly reduce the CO_2-induced sink potential of high-latitude ecosystems, turning all of our simulation experiments into carbon sources by 2100; however, the uncertainty associated with the warming-induced increase in N mineralization is unresolved here. Finally, several other processes, not modeled here, could also affect the high-latitude CO_2 balance, including northerly expansion of the boreal forest (34), changes to the fire regime (10, 35), or other disturbance mechanisms.

We attempted to incorporate in this study some of the latest mechanistic understanding about the mechanisms controlling soil CO_2 respiration and wetland CH_4 emissions, but uncertainties remain large, due to incomplete understanding of biogeochemical and physical processes and our ability to encapsulate them in large-scale models. In particular, small-scale hydrological effects (36) and interactions between warming and hydrological processes are only crudely represented in the current generation of terrestrial biosphere models. Fundamental processes such as thermokarst erosion (37) or the effects of drying on peatland CO_2 emissions (e.g., ref. 38) are lacking here, causing uncertainty on future high-latitude carbon-climate feedbacks. In addition, large uncertainty arises from our ability to model wetland dynamics or the microbial processes that govern CH_4 emissions, and in particular how the complicated dynamics of permafrost thaw would affect these processes.

The control of changes in the carbon balance of terrestrial regions by production vs. decomposition has been explored by a number of authors, with differing estimates of whether vegetation or soil changes have the largest overall effect on carbon storage changes (39–41). These results demonstrate that with the inclusion of two well-observed mechanisms: the relative inhibition of respiration by soil freezing (42) and the vertical motion in Arctic soils that buries old but labile carbon in deeper permafrost horizons, which can be remobilized by warming (3), the high-latitude terrestrial carbon response to warming can tip from near equilibrium to a sustained source of CO_2 by the mid-21st century. We repeat that uncertainties on these estimates of CO_2 and CH_4 balance are large, due to the complexity of high-latitude ecosystems vs. the simplified process treatment used here.

The 61 Pg C reduction in cumulative carbon fluxes at 2100 between our permafrost and control cases imply that when taking frozen soil processes into account, climate change can lead to a large reduction of the carbon sinks in high-latitude. About one third (24 Pg) of this climate-induced carbon loss is due to seasonally frozen soil carbon, the rest being due to permafrost processes. The modeling studies included in the IPCC AR4 (6, 7) inferred that tropical ecosystems would act as a climate change-induced carbon source, mid- and high-latitude ecosystems could be regions where climate change would enhance carbon storage; we show here that including the vast permafrost carbon pool in models leads to a qualitatively different result, in which high latitudes act as future CO_2 and CH_4 sources, leaving only the mid latitudes as potential climate regulators. We note as well that significant permafrost stocks exist and a steep loss continues at 2100, so that beyond the time horizon considered here there is still a potential for enormous carbon losses from high-latitude soils to continue.

ACKNOWLEDGMENTS. We thank Soenke Zaehle for helpful discussion. We thank the circumpolar active layer monitoring (CALM) program and community for making their data publicly available. We thank an anonymous reviewer for comments that improved the paper. This research was supported by the project Impact-Boreal funded by the Agence Nationale pour la Recherche and by the European Union project Comprehensive Modeling of the Earth System for Better Climate Prediction and Projection (COMBINE). Computing support was provided by Commissariat à l'Energie Atomique. This research was supported by the Director, Office of Science, Office of Biological and Environmental Research of the U.S. Department of Energy under Contract No. DE-AC02-05CH11231 as part of their Climate and Earth System Modeling Program.

1. McGuire AD, et al. (2009) Sensitivity of the carbon cycle in the Arctic to climate change. *Ecol Monogr* 79:523–555.
2. Knorr W, Prentice I, House J, Holland E (2005) Long-term sensitivity of soil carbon turnover to warming. *Nature* 433:298–301.
3. Schuur EAG, et al. (2009) The effect of permafrost thaw on old carbon release and net carbon exchange from tundra. *Nature* 459:556–559.
4. Tarnocai C, et al. (2009) Soil organic carbon pools in the northern circumpolar permafrost region. *Global Biogeochem Cycles* 23:GB2023.
5. Friedlingstein P, et al. (2006) Climate-carbon cycle feedback analysis: Results from the C^4MIP model intercomparison. *J Clim* 19:3337–3353.
6. Denman KL, et al. (2007) Couplings between changes in the climate system and biogeochemistry. *Climate Change 2007: The Physical Science Basis. Contribution of Working Group I to the Fourth Assessment Report of the Intergovernmental Panel on Climate Change*, eds S Solomon et al. (Cambridge Univ Press, Cambridge, UK).
7. Meehl GA, et al. (2007) Global climate projections. *Climate Change 2007: The Physical Science Basis. Contribution of Working Group I to the Fourth Assessment Report of the Intergovernmental Panel on Climate Change*, eds S Solomon et al. (Cambridge Univ Press, Cambridge, UK).
8. Sitch S, et al. (2007) Assessing the carbon balance of circumpolar Arctic tundra using remote sensing and process modeling. *Ecol Appl* 17:213–234.
9. Qian H, Joseph R, Zeng N (2010) Enhanced terrestrial carbon uptake in the northern high latitudes in the 21st century from the coupled carbon cycle climate model intercomparison project model projections. *Glob Change Biol* 16:641–656.
10. Zhuang Q, et al. (2006) CO_2 and CH_4 exchanges between land ecosystems and the atmosphere in northern high latitudes over the 21st century. *Geophys Res Lett* 33:L17403.
11. Schaefer K, Zhang T, Bruhwiler L, Barrett AP (2011) Amount and timing of permafrost carbon release in response to climate warming. *Tellus Ser B* 63:165–180.

12. Bousquet P, et al. (2006) Contribution of anthropogenic and natural sources to atmospheric methane variability. *Nature* 443:439–443.
13. Fung I, et al. (1991) 3-Dimensional model synthesis of the global methane cycle. *J Geophys Res Atmos* 96:13033–13065.
14. Forster P, et al. () Changes in atmospheric constituents and in radiative forcing. *Climate Change 2007: The Physical Science Basis. Contribution of Working Group I to the Fourth Assessment Report of the Intergovernmental Panel on Climate Change*, eds S Solomon et al. (Cambridge Univ Press, Cambridge, UK).
15. Koven C, et al. (2009) On the formation of high-latitude soil carbon stocks: The effects of cryoturbation and insulation by organic matter in a land surface model. *Geophys Res Lett* 36:L21501.
16. Khvorostyanov D, Krinner G, Ciais P, Heimann M, Zimov S (2008) Vulnerability of permafrost carbon to global warming. Part I: Model description and role of heat generated by organic matter decomposition. *Tellus Ser B* 60:250–264.
17. Ringeval B, et al. (2010) An attempt to quantify the impact of changes in wetland extent on methane emissions on the seasonal and interannual timescales. *Global Biogeochem Cycles* 24:GB2003.
18. Ringeval B, et al. (2011) Climate-methane feedback from wetlands and its interaction with the climate-carbon cycle feedback. *Biogeosci Discuss* 8:3203–3251.
19. Decharme B (2007) Influence of runoff parameterization on continental hydrology: Comparison between the Noah and the ISBA land surface models. *J Geophys Res Atmos* 112:D19108.
20. Beven K, Kirkby M (1979) A physically based variable contributing area model of basin hydrology. *Hydrol Sci Bull* 24:43–69.
21. Walter B, Heimann M, Matthews E (2001) Modeling modern methane emissions from natural wetlands I. Model description and results. *J Geophys Res (Atmos)* 106:D24.
22. Brohan P, Kennedy J, Harris I, Tett S, Jones P (2006) Uncertainty estimates in regional and global observed temperature changes: A new dataset from 1850. *J Geophys Res (Atmos)* 111:D12106.
23. Sheffield J, Goteti G, Wood EF (2006) Development of a 50-year high-resolution global dataset of meteorological forcings for land surface modeling. *J Clim* 19:3088–3111.
24. Marti O, et al. (2006) The new IPSL climate system model: IPSL-CM4. (Institut Pierre Simon Laplace des Sciences de l'Environnement Global, Paris).
25. Brown J, Hinkel K, Nelson F (2000) The circumpolar active layer monitoring (CALM) program: Research designs and initial results. *Polit Geogr* 24:165–258.
26. Beer C, et al. (2010) Terrestrial gross carbon dioxide uptake: Global distribution and covariation with climate. *Science* 329:834–838.
27. Cadule P, et al. (2010) Benchmarking coupled climate-carbon models against long-term atmospheric CO_2 measurements. *Global Biogeochem Cycles* 24:GB2016.
28. Riordan B, Verbyla D, McGuire AD (2006) Shrinking ponds in subarctic Alaska based on 1950–2002 remotely sensed images. *J Geophys Res* 111:G04002.
29. Smith L, Sheng Y, MacDonald G, Hinzman L (2005) Disappearing Arctic lakes. *Science* 308:1429–1429.
30. Bonan GB, Levis S (2010) Quantifying carbon-nitrogen feedbacks in the Community Land Model (CLM4). *Geophys Res Lett* 37:L07401.
31. Zaehle S, Friedlingstein P, Friend AD (2010) Terrestrial nitrogen feedbacks may accelerate future climate change. *Geophys Res Lett* 37:L01401.
32. Waelbroeck C, Monfray P, Oechel W, Hastings S, Vourlitis G (1997) The impact of permafrost thawing on the carbon dynamics of tundra. *Geophys Res Lett* 24:229–232.
33. Mack M, Schuur E, Bret-Harte M, Shaver G, Chapin F (2004) Ecosystem carbon storage in Arctic tundra reduced by long-term nutrient fertilization. *Nature* 431:440–443.
34. Euskirchen E, McGuire A, Chapin F, III, Yi S, Thompson C (2009) Changes in vegetation in northern Alaska under scenarios of climate change, 2003–2100: Implications for climate feedbacks. *Ecol Appl* 19:1022–1043.
35. Carrasco JJ, Neff JC, Harden JW (2006) Modeling physical and biogeochemical controls over carbon accumulation in a boreal forest soil. *J Geophys Res (Biogeosci)* 111:G02004.
36. Bohn TJ, Lettenmaier DP (2010) Systematic biases in large-scale estimates of wetland methane emissions arising from water table formulations. *Geophys Res Lett* 37:L22401.
37. van Huissteden J, et al. (2011) Methane emissions from permafrost thaw lakes limited by lake drainage. *Nat Clim*, 1 pp:119–123.
38. Ise T, Dunn AL, Wofsy SC, Moorcroft PR (2008) High sensitivity of peat decomposition to climate change through water-table feedback. *Nat Geosci* 1:763–766.
39. Matthews HD, Eby M, Ewen T, Friedlingstein P, Hawkins BJ (2007) What determines the magnitude of carbon cycle-climate feedbacks? *Global Biogeochem Cycles* 21:GB2012.
40. Friedlingstein P, Dufresne J, Cox P, Rayner P (2003) How positive is the feedback between climate change and the carbon cycle? *Tellus Ser B* 55:692–700.
41. Jones C, Cox P, Huntingford C (2003) Uncertainty in climate-carbon-cycle projections associated with the sensitivity of soil respiration to temperature. *Tellus Ser B* 55:642–648.
42. Goulden M, et al. (1998) Sensitivity of boreal forest carbon balance to soil thaw. *Science* 279:214–217.

Supporting Information

Koven et al. 10.1073/pnas.1103910108

SI Text

Model and Experimental Setup. The vertical discretization of soil temperature and soil carbon in this version of ORCHIDEE uses a 32-layer exponential grid, with a maximum depth of 51.2 m. At each timestep, soil carbon is input from a fraction of decomposed litter following standard ORCHIDEE (1), and vertically discretized to an exponential profile with e-folding depth based on the plant functional type-specific rooting depth profile. Where permafrost layers exist, soil carbon inputs are set to zero below the permafrost table, and the total profile is adjusted so that the integral of carbon inputs to the active layer is conserved. The temperature-dependant soil carbon residence time is based on the standard ORCHIDEE scheme, which follows the CENTURY model (2), except that it is calculated separately for each soil layer based on the temperature at that layer.

For the Arctic region, we assume that temperature is the dominant physical control on decomposition (3, 4), and thus the only moisture limitations to soil carbon respiration are those that accompany freezing. For the freeze and subsequent experiments, we parameterize the liquid moisture control on decomposition by modifying the temperature dependence of respiration in frozen soils. Respiration thus becomes lower than in our control case, in which we use only a constant Q_{10} of 2 throughout the temperature range. A variety of frozen respiration functions have been proposed (5, 6), for example spanning Q_{10} range from 10^2 to 10^6 (5). Here we perform four separate sensitivity experiments (Fig. S2): two with a second exponential with Q_{10} values and two with a linear drop off between the fixed respiration rate at 0 °C and a T_{crit} where respiration goes to 0. For the Q_{10} experiments, we use Q_{10} of 100 and 1,000 for temperatures below 0 °C; for the T_{crit} experiments, we use T_{crit} values of −1C and −3C. We report the mean and standard deviation of all four sets of runs for the freeze experiment; for the heating, and permafrost experiments we use a T_{crit} of −1C.

For the permafrost experiment, we perform a sensitivity test to the vertical diffusion constant that we use to model processes such as cryoturbation that transport organic material from surface or active layer into the permafrost layers of the soil. The rate of such diffusion is poorly known, however radiocarbon dates of subducted organic material (7) suggest a centennial to millennial timescale. Thus we try to bracket this range, with diffusion constants of 1 e–2 m^2/y and 1 e–3 m^2/y.

For the heating experiment, we also try to bracket the range of potential values for the exothermic heat release term described by Khvorostyanov et al. (8). We implicitly use a value of zero for all prior experiments (control, freeze, and permafrost); for the heating experiment, we additionally test the model with values of 20 and 40 MJ/kg C, which covers the range used by Khvorostyanov et al. (8).

The surface carbon stocks are initialized iteratively for 10,000 y as described by Koven et al. (9). For the simulations that involve permafrost carbon, i.e. permafrost and heating, we also include carbon in deeper soil layers where yedoma soils exist in Eastern Siberia. We define the yedoma geographic extent following Walter et al. (10); we use initial yedoma carbon concentrations of 17.6 Kg C/m^3 following Zimov et al. (11) and a bulk lability set by partitioning the yedoma carbon between the three ORCHIDEE carbon lability pools to match the carbon residence time of the 5 °C soil incubation data of Dutta et al. (12).

Mean and error estimates for the freeze, permafrost, and heating experiments are found as the mean and standard deviation of an ensemble of model runs with varied parameter values. For each ensemble member, a chosen parameter value is used in the initial model equilibration and for the subsequent transient experiments (control, CO_2-only, CO_2+climate). For the freeze experiment, we vary the frozen respiration function; for the permafrost experiment, we vary the soil organic matter (SOM) vertical diffusion constant; and for the heating experiment, we vary the exothermic heat per unit carbon consumption term.

Comparison of modeled and observed carbon stocks. A strong difference between the experiments tested here is seen in the size of the carbon stocks that are initially in equilibrium with the model (Fig. S4 and Table S1), where inclusion of the freeze-induced inhibition of respiration leads to larger equilibrium soil carbon stocks and brings the model in closer agreement with inventories of high-latitude soil carbon in the northern circumpolar soil carbon database (NCSCD) (13). This increase in SOM C stocks is particularly true in the Eastern Siberian region, where high carbon stocks are associated with cryoturbated permafrost-affected soils (turbels). Because peat formation processes are not included in ORCHIDEE, we strongly underestimate the substantial carbon stocks associated with peat deposits, particularly those in western Siberia and Canada.

The large increase in initial high-latitude soil C stocks (from ∼200 Pg to ∼500 Pg C in the top 3 m of soil) demonstrates the large sensitivity of ecosystem carbon storage to the representation of soil processes in the model, despite these effects having only a weak influence on the behavior of the modeled carbon fluxes on interannual-to-seasonal timescales due to the slow response time of the soil C pool.

Sensitivity of results to model parameters and processes. For the ensemble of runs performed with different frozen respiration functions, initial carbon stocks ranged 246 to 264 for the top 1 m of soils, with larger carbon stocks associated with lower frozen respiration rates. Lower respiration rates also translated to higher sensitivity of the carbon pools to warming, with a standard deviation of 3 Pg between the ensemble members.

For the permafrost experiment, we vary the vertical diffusion constant by an order of magnitude. For the faster diffusion case ($k = 10^{-2}$ m/y), total carbon stocks are larger than the slower diffusion case ($k = 10^{-3}$ m^2/y) after the initial 10,000 y spin up period due to faster equilibration between the active layer carbon and permafrost carbon. In addition, the lability of the permafrost carbon was higher, with a higher proportion of active pool to slow pool carbon in the permafrost layers. This increased lability leads to a higher vulnerability of the permafrost carbon stocks to warming, and thus higher loss rates (69 Pg vs. 55 Pg, respectively).

For the permafrost experiment, deeper carbon stocks act as only a weak source of methane (approximately 1 Tg/y), because the grid cells with yedoma are only in the coldest parts of Siberia, which do not completely thaw during the time horizon considered here. Shallower permafrost carbon does not act as a strong methane source; because we assume here that only the active carbon pool is available as a substrate for methanogenesis, the residence time of this carbon is short relative to its mixing time by cryoturbation, and thus the stock of this pool is minor relative to the wetland sources.

We perform two scenarios with nonzero values of the microbial heat release term: 20 MJ/kg C and 40 MJ/kg C. The overlap with the error shading in Fig. 2*B* between the lower range of the heating case and the upper range of the permafrost case is due to the fact that the middle estimate of the microbial heat release

parameter leads to only a minor change in the model behavior, it is only the upper estimate, in which the heat released is enough to lead to further thaw of deeper permafrost, that large carbon emissions occur.

Our results also show that the heat release from organic carbon decomposition can increase both the CO_2 and CH_4 release. The idea of microbial heat release playing a role in permafrost carbon cycling was first proposed in ref. 14. This idea has strong theoretical justification—in that thermodynamics dictates that the energy differential between organic substrate and inorganic carbon will eventually become thermal energy—and is supported by some field evidence (15). The actual quantity of heat released per unit carbon respired (H) is not well constrained (here we vary H between 0 and 40 MJ/kg C) (8), and more investigation is needed to determine the strength of this mechanism in actual permafrost soils. In particular, this mechanism has a very weak effect on the steady-state dynamics of the model (Fig. S4); instead it only becomes important when the system is perturbed out of equilibrium. Thus we cannot reject the hypothesis that microbial heat production could affect the carbon balance, as obtained in local field experiments (15). However, we note that the heating process has a strong threshold behavior relative to the heat release parameter H, (8) and only acts to create a significant extra source of CO_2 if the parameter H is above 20 MJ/kg C. Therefore, this process will only be important if the heat release is at the upper end of what is thermodynamically possible, and in this case the model present-day carbon balance falls out of agreement with estimates of the high-latitude carbon balance; because of the strong threshold behavior, lack of quantitative observations at the appropriate scale, and overall large uncertainty of this process, we instead consider the permafrost case, which does not include the heating term, our best estimate.

The large source of CO_2 and CH_4 that results from climate change in the model experiment with the upper estimate of microbial heat decomposition is qualitatively similar to that described by Khvorostyanov et al. (8): In certain grid cells, the heat released results in a positive feedback that leads to thawing to the base of the C-rich soil (25 m). In reality, however, the impact of a biological heat source in soils may be quite different. A particular simplification inherent in this modeling framework is that we model heat transfer as 1-D heat conduction; real soils will have 3-D heat transport, and advection of heat by groundwater and vapor flow may be critical to the thawing processes (16). However, although these processes may damp any positive feedback loops such as the one we calculate here for the microbial heat release experiment, they may also act to destabilize and accelerate thaw through processes such as thermokarst.

The wetland CH_4 results are calculated with the ORCHIDEE-WET model (17, 18), separately, forced by the same scenario, and added to the CH_4 emissions from the permafrost model. The CH_4 submodel of ORCHIDEE-WET is based on the Walter et al. (19) CH_4 model, in which methanogenesis, methanotrophy, and CH_4 transport are calculated for saturated soil columns (17, 18) The temperature sensitivity of methanogenesis for a given substrate availability in Walter et al. (19) and ORCHIDEE-WET is based on a modified Q_{10} formulation:

$$g = f(T(t,z))Q_{10}^{T(t,z)-T_{\text{mean}}}, \qquad \textbf{[S1]}$$

where $f(T)$ is a step function that halts methanogenesis in frozen soils, and the term T_{mean} is the location-dependant mean annual temperature. In the original Walter et al. (19) formulation, Q_{10} was set to 6; here it is set to 3 based on an optimization of the model at several sites and against global inversions, as described by Ringeval et al. (17). In addition, we test alternate hypotheses about microbial adaptation to climate change to assess the uncertainty associated with adaptation to climate change, by allowing T_{mean} to vary or stay fixed.

In addition to the sensitivity to T_{mean}, the wetland CH_4 model is run with separate experiments allowing the soil C (which is used as a proxy for the methanogenesis substrate) to evolve with time, and held constant at preindustrial values (Table S2). Similarly, separate varying and constant experiments are done with the modeled wetland extent. The results demonstrate a high sensitivity of the model to these processes, with multiple local feedback mechanisms, including a sensitivity of the wetland fraction to transpiration fluxes via both CO_2 fertilization and climate change. More discussion of these mechanisms is in ref. 18.

1. Krinner G, et al. (2005) A dynamic global vegetation model for studies of the coupled atmosphere-biosphere system. *Global Biogeochem Cycles* 19:GB1015.
2. Parton W, Stewart J, Cole C (1988) Dynamics of C, N, P, and S in grassland soils—a model. *Biogeochemistry* 5:109–131.
3. Hobbie SE, Schimel JP, Trumbore SE, Randerson JR (2000) Controls over carbon storage and turnover in high-latitude soils. *Glob Change Biol* 6:196–210.
4. Goulden M, et al. (1998) Sensitivity of boreal forest carbon balance to soil thaw. *Science* 279:214–217.
5. Monson R, et al. (2006) Winter forest soil respiration controlled by climate and microbial community composition. *Nature* 439:711–714.
6. Mikan CJ, Schimel JP, Doyle AP (2002) Temperature controls of microbial respiration in arctic tundra soils above and below freezing. *Soil Biol Biochem* 34:1785–1795.
7. Kaiser C, et al. (2007) Conservation of soil organic matter through cryoturbation in Arctic soils in Siberia. *J Geophys Res (Biogeosci)* 112:G02017.
8. Khvorostyanov D, Krinner G, Ciais P, Heimann M, Zimov S (2008) Vulnerability of permafrost carbon to global warming. Part I: Model description and role of heat generated by organic matter decomposition. *Tellus Ser B* 60:250–264.
9. Koven C, et al. (2009) On the formation of high-latitude soil carbon stocks: The effects of cryoturbation and insulation by organic matter in a land surface model. *Geophys Res Lett* 36:L21501.
10. Walter KM, Edwards ME, Grosse G, Zimov SA, Chapin FS, III (2007) Thermokarst lakes as a source of atmospheric CH_4 during the last deglaciation. *Science* 318:633–636.
11. Zimov S, et al. (2006) Permafrost carbon: Stock and decomposability of a globally significant carbon pool. *Geophys Res Lett* 33:L20502.
12. Dutta K, Schuur EAG, Neff JC, Zimov SA (2006) Potential carbon release from permafrost soils of Northeastern Siberia. *Glob Change Biol* 12:2336–2351.
13. Tarnocai C, Swanson D, Kimble J, Broll G (2007) Northern Circumpolar Soil Carbon Database. (Research Branch, Agriculture and Agri-Food Canada, Ottawa).
14. Zimov S, et al. (1996) Siberian CO_2 efflux in winter as a CO_2 source and cause of seasonality in atmospheric CO_2. *Clim Change* 33:111–120.
15. Zimov SA, et al. (2006) Permafrost carbon: Stock and decomposability of a globally significant carbon pool. *Geophys Res Lett* 33:L20502.
16. Kane D, Hinkel K, Goering D, Hinzman L, Outcalt S (2001) Nonconductive heat transfer associated with frozen soils. *Global Planet Change* 29:275–292.
17. Ringeval B, et al. (2010) An attempt to quantify the impact of changes in wetland extent on methane emissions on the seasonal and interannual time scales. *Global Biogeochem Cycles* 24:GB2003.
18. Ringeval B, et al. (2011) Climate-methane feedback from wetlands and its interaction with the climate-carbon cycle feedback. *Biogeosci Discuss* 8:3203–3251.
19. Walter B, Heimann M, Matthews E (2001) Modeling modern methane emissions from natural wetlands I. Model description and results. *J Geophys Res (Atmos)* 106:D24.

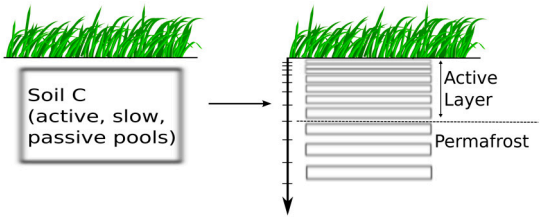

Fig. S1. Schematic of model structure: Vertically integrated soil C pools have been replaced by an explicit vertical discretization of soil carbon, and coupling with permafrost dynamics. In the freeze and subsequent experiments, soil carbon turnover time is dramatically increased in frozen soil layers. In the permafrost experiment, soil carbon is mixed from the active layer into permafrost layers during spin up, leading to a buildup of soil carbon in frozen layers.

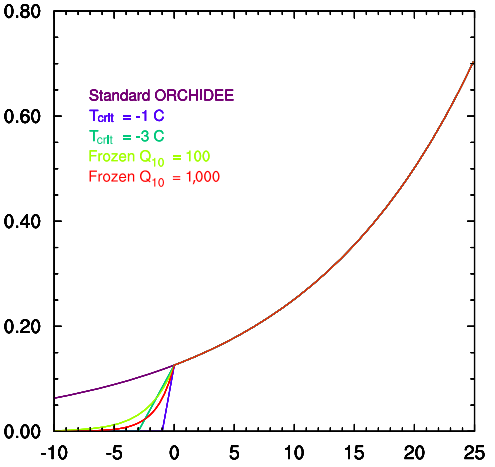

Fig. S2. Modeled frozen respiration functions. All follow the standard ORCHIDEE respiration control function ($Q_{10} = 2$) for unfrozen soils; two curves follow a second exponential function ($Q_{10} = 100, 1,000$) for frozen soils, and two use a linear drop off to zero respiration at a temperature $T_{crit} = -1$ or -3 C.

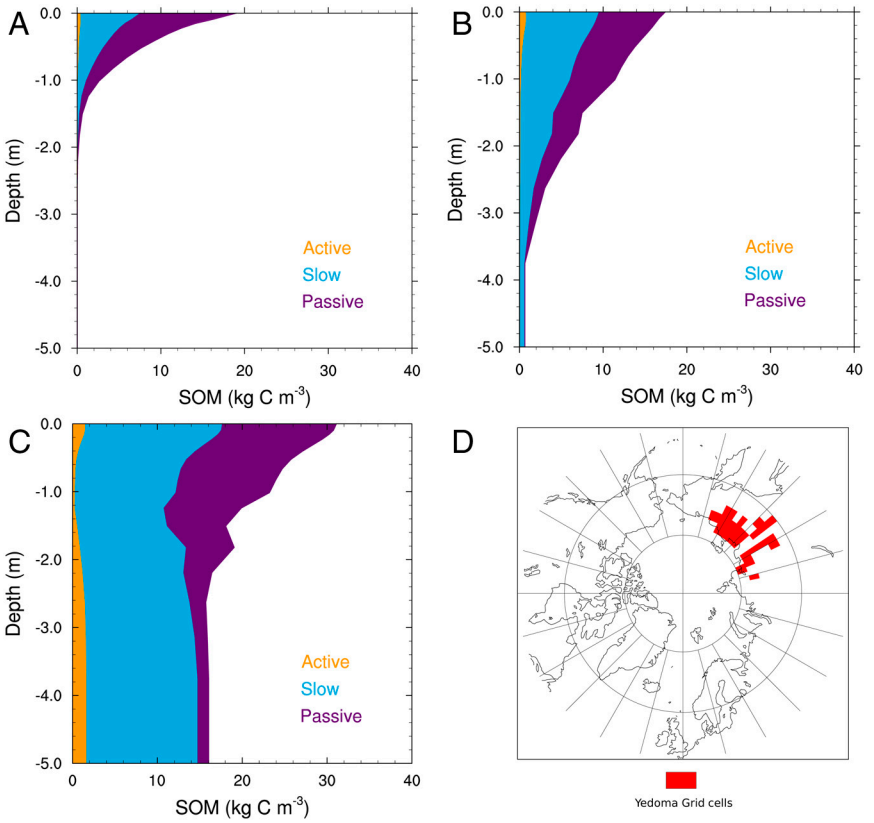

Fig. S3. Modeled soil C vertical profiles. (*A*) Mean over all permafrost grid cells in freeze case. (*B*) Mean over permafrost grid cells in permafrost case. (*C*) Mean over all yedoma grid cells in permafrost case. (*D*) Map of grid cells where yedoma is initialized to be present.

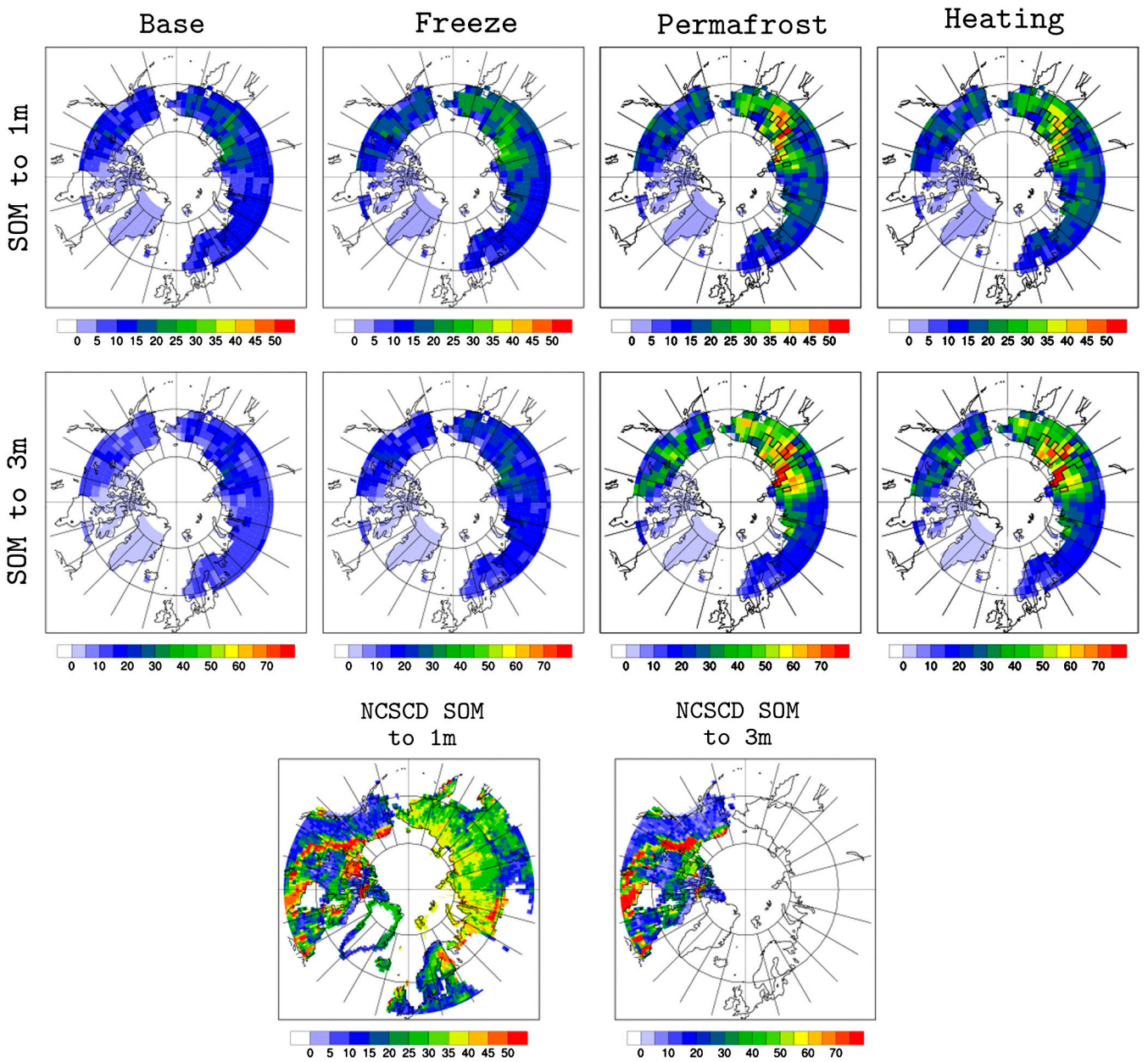

Fig. S4. Maps of initial soil carbon (kg C/m2) to depths of 1 m and 3 m for each experiment, and for comparison, observations from the NCSCD (13). Outlined grid cells in permafrost and heating experiments are those where yedoma carbon stocks are present in model.

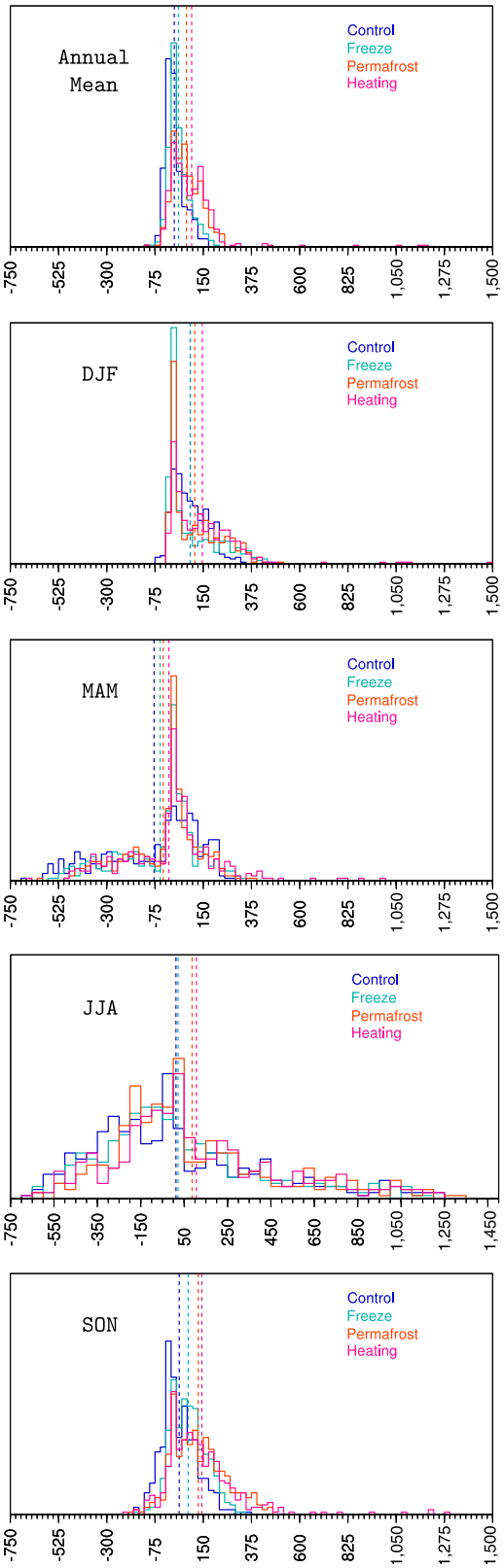

Fig. S5. Histograms of CO_2 balance for each case at the end of the modeled period (gC/m2/y), for annual mean and for each season.

Table S1. List of experiments presented here, with description of processes added in each experiment, parameter ranges tested, and total CO_2 flux resulting from climate change alone at end of each experiment

Experiment Name	Processes included	Parameters varied and range tested	Initial soil carbon stock for region north of 60°N to 1 m (Pg)	Initial soil carbon stock for region north of 60°N to 3 m (Pg)	Integrated net CO_2 flux 1860–2100 due to:		
					CO_2 (Pg)	CO_2+climate change (Pg)	Climate change (Pg)
Control	Standard ORCHIDEE + vertical discretization of soil carbon; improved snow insulation and ice latent heat		191	211	−69	−68	1
Freeze	Control + inhibition of soil C decomposition when frozen	Frozen respiration function (see Fig. S2 for functions tested)	254	280	−81 + −2	−56 + −1	25 + −3
Permafrost	Freeze + insulation by SOM, vertical mixing of soil carbon, and yedoma	Cryoturbation diffusion constant k : .01 – .001 m^2/y	306	504	−88 + −1	−27 + −7	62 + −7
Heating	Permafrost + exothermic heat release with decomposition	Exothermic heat release H : 20–40 MJ/kg C	294	476	−80 + −2	4 + −18	85 + −16

Table S2. Influence of different terms of CH_4 budget

Increase of wetlands CH_4 emissions (Tg/y) in 2090–2100 in comparison to preindustrial emissions	CH_4 flux densities		Wetland extent	CO_2	CO_2+Climate	Climate
	Q_{10}	Soil carbon				
	3	F	F	+68	**+25**	−43
	3	F	PI	**+40**	**+83**	+43
	3	PI	F	+15	+19	+4
	3	PI	PI	+1	+59	+58
Increase of CH_4 emissions (Tg/y) linked to permafrost in comparison to preindustrial emissions	Permafrost case			0	+0.5	+0.5
	Heating case			0	+14	+14

CH_4 in ORCHIDEE arise from two separate submodels, a wetland source and a permafrost source. We apply different parameter and process sensitivities for the different sources, shown here as separate lines. The three columns on the right show the model high-latitude CH_4 emission changes (relative to a baseline of 33 Tg/y) due to changes in CO_2, total change due to CO_2 and climate, and the change due to climate alone (difference between first two columns). To assess the sensitivity of the CH_4 model to different processes, the model is run allowing the methanogenesis substrate to vary freely with the climate or to stay fixed (F) at preindustrial (PI) values. Separate F and PI runs are also done with the wetland extent. The three bold numbers refer to the panels in Fig. 4. T_{mean} is held constant for all the experiments listed here.